Journal of Sustainable Development of Smart Energy Networks
https://www.sdewes.org/jsdsen

Year 2026, Volume 1, Issue 1, 2030684

Original Research Article

Environmentally Driven Optimization of Residential BEV Charging Using Time-Varying Power Grid CO_2 Emission Factors

Ilenia Perugini*[*1], E. Marrasso[1], C. Martone[1], G. Pallotta[1], C. Roselli[1], M. Sasso[1]
[1]Department of Engineering, University of Sannio, Benevento, Italy
e-mail: i.perugini@studenti.unisannio.it, marrasso@unisannio.it, cmartone@unisannio.it, giopallotta@unisannio.it, croselli@unisannio.it, sasso@unisannio.it

Cite as: Perugini, I., Marrasso, E., Martone, C., Pallotta, G., Roselli, C., Sasso, M., Environmentally Driven Optimization of Residential BEV Charging Using Time-Varying Power Grid CO_2 Emission Factors, J. sustain. dev. smart. en. net., 1(1), 2030684, 2026, DOI: https://doi.org/10.13044/j.sdsen.d3.0684

ABSTRACT

The widespread adoption of battery electric vehicles is widely recognized as a key strategy for reducing emissions in the transport sector. However, the environmental benefits of electric mobility strongly depend on the temporal variability of the electricity generation mix and its associated emission intensity. This study investigates the potential of optimizing vehicle charging schedules based on time-varying carbon dioxide emissions factor, rather than grid-oriented criteria, to further reduce the indirect emissions linked to the operation of electric vehicle charging. To this end, an environmentally driven charging optimisation algorithm is developed, explicitly accounting for both the hourly variability of grid emission factors, derived from processing historical real Italian electricity production data, and the air temperature-dependent energy consumption of the BEV. The proposed framework is applied to a representative residential charging scenario, assuming overnight charging. Within this predefined charging window, the optmisation algorithm allocates the required charging energy over time so as to minimise the total carbon dioxide emissions. Results show that emission-aware charging strategies can reduce annual carbon dioxide emissions by approximately 5–6% compared to conventional uncontrolled charging, while ensuring that the vehicle is always fully charged and ready for use at the predefined departure time. In addition, by its design, the proposed environmentally driven charging optimization features as a scalable structure that can be integrated with existing smart charging strategies, contributing to the decarbonization of the transport sector.

KEYWORDS

Electric vehicles, Energy consumption factor, Carbon dioxide emissions, Electricity generation mix, Charging optimization, Vehicle-to-grid flexibility, Transport electrification.

INTRODUCTION

Over the last few decades, the European Union (EU) has introduced several directives and regulations to address climate change. In detail, the UE, through the Green Deal, sets up the ambitious goal to decarbonize end-users' energy demand by 2050 [1], [2]. Among the different energy sectors, the transport sector stands out as one of the most polluting due to its heavy reliance on fossil fuels. In fact, fossil oil accounted for about 91% of final energy demand, a value only 3.5% lower than in the 1970s [2]. As a result, the transport sector is responsible for more than one-quarter of the total carbon dioxide (CO_2) emissions in Europe [3]. In addition, since 1990, it has been the only sector whose CO_2 emissions have been increasing, with road

* Corresponding author

transport driving most of this increase [2]. The only significant reduction was observed during the COVID-19 pandemic due to mobility restrictions introduced to limit the spread of the virus [4]. More specifically, passenger and cargo transport are responsible for about 60.6% and 27.1%, respectively, of the total CO_2 emissions from road transport [3].

The data reported above underscores the need for effective action in the transport sector. To this end, the EU has identified the use of alternative fuels as one key option to cut transport-related emissions [5]. In addition, throughout the Directive 2014/94/EU [6] and Regulation 631/2019 [7], it paves the way for the rollout of Electric Vehicles (EVs). Regulation 631/2019 establishes the CO_2 emissions limits for the new registration of cargo and commercial light vehicles, set at 95 gCO_2/km and 147 gCO_2/km, respectively, by 2020. Regulation provided more stringent progressive thresholds; however, with the introduction of Regulation 851/2023 [8], which is part of the Fit for 55% packages [9], these thresholds are becoming increasingly stringent. The update regulation aims to phase out the registration of new fossil-fuel-powered internal combustion engine and hybrid electric vehicles by 2035. Consequently, only the new registrations of Battery Electric Vehicles (BEVs) and Fuel Cell Electric Vehicles (FCEVs) will be allowed. Since the implementation of the updated regulation requires deep technological and industrial change, many concerns about the feasibility and timing of this target have arisen, which could postpone the deadline of this binding limit [8].

As a consequence of this ongoing evolution in the vehicle's CO_2 emissions, increasing attention has been given to the topic in academic literature. The results carried out by the wide assessments conducted demonstrate that electrification of the transport sector could play a key role in decarbonizing this hard-to-abate sector, but its actual impact depends on several circumstances, such as the carbon intensity of the electricity mix, charging strategies, and CO_2 prices [9]–[11]. Beyond the potential reduction in CO_2 emissions, other advantages have been investigated. For example, the powertrain of EVs is more efficient compared with that of an Internal Combustion Engine Vehicle (ICEV); since the absence of the combustion process and the zero tailpipe exhaust gases, the spread of EVs contributes to reducing noise pollution, and improving the air quality [12]. All these aspects are particularly relevant for urban areas, where there is a concentration of circulating vehicles near pedestrians.

Side Effects of Adopting BEV and the Literature Gap

Summarizing the examined literature, one key outcome clearly emerges: the adoption of BEVs has the potential to reduce CO_2 emissions in the transport sector; however, this outcome is not guaranteed. In several cases, BEV may even lead to an increase in CO_2 emissions. It depends on several critical factors, which are detailed below. Therefore, the key question is not *whether* BEVs could be useful, but *how* their deployment should be managed to avoid the side effects of their adoption. Some of the main issues identified in the literature and side effects are summarized below:

a) The decrease in CO_2 emissions is strictly linked to the carbon intensity of the power grid. The battery charging represents an additional pure electric load that will be met by the electricity withdrawn from the power grid. Consequently, the first side effect is the risk that BEV adoption leads not to a reduction in CO_2 emissions, but rather their shift from the vehicle tailpipe to the power plant [13], [14]. The straightforward solution proposed in the literature is, trivially, to increase the RES (Renewable Energy Source) energy conversion systems penetrations [10]. Nevertheless, the electricity generation from renewable-based plants is neither temporally nor geographically constant. As demonstrated by [15], this is one of the causes of the temporal and spatial variability in the carbon emission factor of the power grid. Most works neglect one or both dimensions of this variability. Several works rely on static carbon emissions factors, differentiated by technology, retrieved from sectoral databases [9], [10], [16]. Other studies focus on the global national amount of CO_2 emissions of different countries, without capturing the hourly dynamics [12]. Time variability is partially addressed in

[11] throughout the bulk power simulation, but spatial variability is not considered. More advanced scenarios are proposed in [17], where time variability is incorporated by solving a unit commitment problem using statistical data retrieved from sectoral databases, rather than real hourly data.

b) Without controlled battery charging strategies, such as vehicle-to-grid strategies (V1G and V2G), the adoption of BEV could enhance:

   1. The instability of the grid due to the risk of concentration of a high electricity demand during specific time windows, especially in residential contexts, where charging often takes place after working hours [18];
   2. The indirect CO2 emissions associated with the battery charging process, if the charging occurs when the productivity of the RES-based plant is lower or when the system is powered by an inefficient and highly polluting fossil fuel power plant, such as coal-fired units [11], [19].

c) The energy required by a battery to travel a given distance depends on several factors, including vehicle characteristics, the road and traffic conditions, i.e., traffic speed and density, transit stops, the design of the city, driving behavior, and the weather conditions, such as air temperature and humidity, as well as precipitation [20], [21]. Therefore, the energy consumption factor is not constant over time. Despite the extensive literature on individual aspects of BEV energy consumption, to the best of the authors' knowledge, no comprehensive assessment has been conducted that encompasses all these aspects. Only [9] considers the traffic conditions through an agent-based modelling, but it does not account for the temperature effects, even though temperature dependency has been widely analyzed in dedicated studies [22], [23].

Novelty

The paper aims to address some of the gaps outlined in the previous section by proposing a more comprehensive methodology to minimize the indirect CO_2 emissions associated with BEV charging. The environmental impact of battery charging is assessed using the well-known Well-to-Wheel (WTW) approach, which splits total CO_2 emissions into two distinct phases: Well-to-Tank (WTT) and Tank-to-Wheel (TTW) [21]. In the case of BEVs, the TTW phase results in zero CO_2 emissions because no combustion occurs during vehicle operation; in contrast, the WTT is the critical step for assessing the environmental performance of BEVs. In general, WTT CO_2 emissions account for the processes required for the production and distribution of the fuel. In the case of BEVs, the literature mainly focuses on the CO_2 emissions from electricity generation at the power plant level [9], [14], [16]. Building on the issues discussed in point (a), the hourly carbon emission factor for BEV charging is calculated, considering real data from the Italian power grid's generation mix. This approach enables the capture of temporal variability in grid carbon intensity and assesses how charging flexibility can be utilized to reduce indirect CO_2 emissions.

With reference to point (b), the paper proposes a new perspective on smart charging strategies. Generally, V1G and V2G refer to a flexible and smart charging in which the user or the owner of the charging infrastructure adjusts the charging time and power according to grid-oriented signals. In particular, V2G enables BEVs to act as a distributed Battery Energy Storage System (BESS), supporting services such as black start capacity and spinning reserve [24]. In contrast, this work proposes an environmentally driven smart charging strategy, referred to as $V1G_{CO2}$. Under this approach, the charging process is scheduled within a predefined time window by prioritizing hours characterized by the lowest grid carbon emission factor, rather than by grid operational constraints or services. It is worth noting that the proposed emission-based charging strategy is conceptually different from price-based approaches, as it explicitly targets minimising indirect CO_2 emissions rather than economic

costs. However, the two strategies may be regarded as complementary, since hours characterised by lower electricity prices often coincide with lower-emission hours, as renewable-based generation typically exhibits low or near-zero marginal costs.

Finally, addressing point (c), this study explicitly accounts for the dependence of BEV energy consumption on ambient temperature. Starting from the energy consumption data made available by the vehicle manufacturer, a regression model is developed to describe the energy consumption rate of the selected BEV as a function of outside temperature [25]. This allows the charging demand to be estimated more accurately over time, improving the consistency between vehicle energy needs and the assessment of charging-related emissions.

Aim and Structure of Paper

The paper aims to develop an environmentally driven optimization strategy for BEV charging, focusing on domestic charging after working hours. The primary objective is to minimize indirect CO_2 emissions by scheduling the charging process during periods when the power grid's carbon emission factors are at their lowest, while ensuring vehicle readiness at the beginning of the following day. The methodology combines real hourly emissions factors for the Italian power grid with temperature-dependent vehicle energy consumption.

The remainder of the paper is structured as follows: Section 2.1 describes the user profile, the charging time window; in Section 2.2 a brief overview of the Italian BEV market in Italy is presented, along with a description of the BEV model used, including the regression used to estimate its energy consumption as a function of the outside temperature; finally the Section 2.3 and 2.4 provide an overview of the carbon emission factor for the Italian power grid and the optimization algorithm adopted to schedule the charging process.

MATERIALS AND METHODS

In this section, the methodology used to assess the environmental impact of domestic BEV charging and its environmentally driven optimisation is presented. The proposed approach is organized as a sequence of interconnected steps that together enable the estimation of charging-related CO_2 emissions. It is structured in three main steps:

- First, a representative user profile is defined to identify the main boundary condition of the problem, including geographical location and exploitable charging infrastructure. It is essential to define the characteristics of the users under assessment to identify the time window available for recharging EVs.
- The energy demand associated with the vehicle used is computed by means of modelling the BEV energy consumption rate as a function of external conditions. In particular, the temperature dependency is considered to capture daily and seasonal variability in the charging needs performance of the BEV. Building upon this, the energy required for each charging session is calculated.
- Finally, the charging process is scheduled within the available time window using an optimization algorithm that allocates energy to time slots (based on 15 minutes) characterized by lower power grid CO_2 emissions factors. The resulting charging profiles are used to compute the indirect CO_2 emissions associated with BEV charging and to compare optimized and non-optimized charging strategies.

A schematic representation of the methodology followed is reported in **Figure 1**.

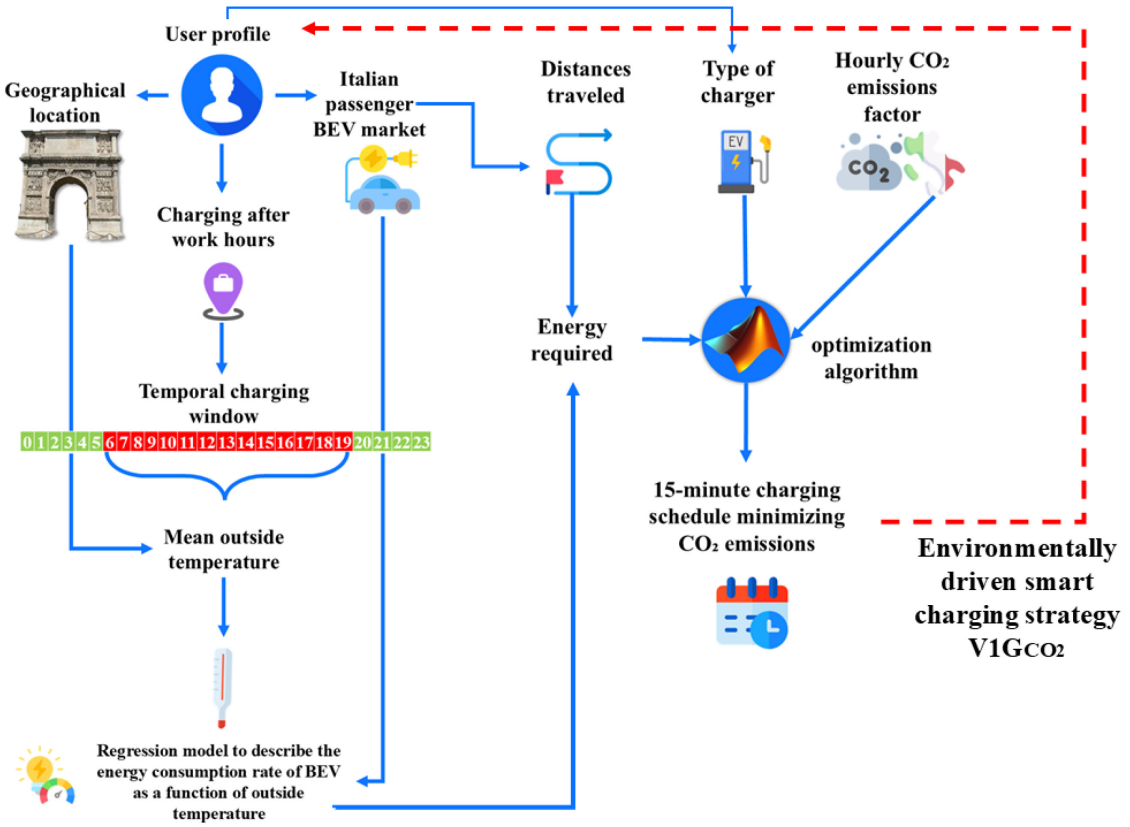

Figure 1. Schematic representation of the methodology followed

User's Profile

The assessment focuses on domestic users who mainly charge their BEV after working hours. According to the outcomes reported by RSE (Ricerca Sistema Energetico), the probability of returning home peaks around 7:00 PM, while it becomes very low around 5:00 AM, [18]. Based on these observations, the time window for vehicle charging is set between 8:00 PM and 5:00 AM of the following day.

A further key aspect of the analysis is the geographical location in which the user drives the BEV. As reported in Section 1.1, the energy consumption factor of EVs is strongly influenced by the outdoor air temperature. The case study focuses on the city of Benevento, situated in the region of Campania in southern Italy. Benevento lies at an altitude of 135 m above sea level, falls within climatic zone C, and has a typical Mediterranean climate. Since the temporal charging windows chosen, the use of BEV is supposed to take place from 6:00 AM to 7:00 PM, therefore, for the influence of temperature, the mean of hourly temperature value, for the year 2023, retrieved by PVGIS [26], belonging to the temporal range from 6:00 AM to 7:00 PM, is computed. The decision to compute the average temperature rather than using hourly temperature data is due to the lack of information on the BEV's actual driving schedule. The information retrieved by [18] allows only for the identification of a plausible daily usage time frame rather than an exact hourly driving pattern; therefore, an average temperature over the assumed driving period is adopted.

Figure 2 presents a graphical representation of daily BEV usage and the domestic charging framework. Driving hours (06:00 AM – 7:00 PM, day d) are used to compute the mean outdoor air temperature, which is later used to estimate the vehicles' energy consumption. The charging process, indicated by green blocks, is allowed only within the domestic charging window (8:00 PM–5:00 AM, day d to day d+*1*).

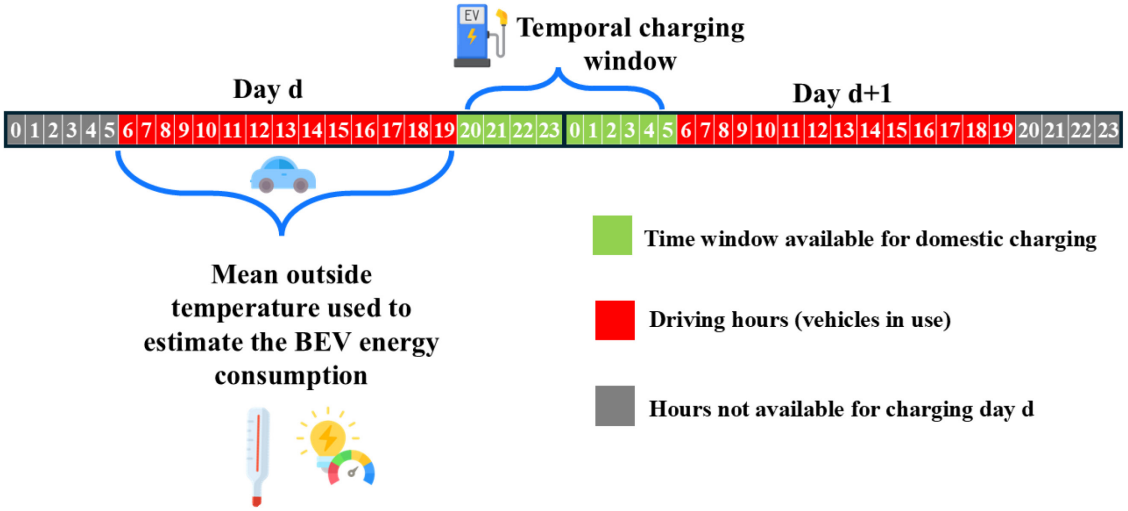

Figure 2. Schematic representation of the daily BEV usage and domestic charging framework

The distance travelled by the user is another key factor, as it directly affects the electricity required to cover a given route. To define the daily driving distances, a study conducted by the National Union of Foreign Vehicle Representatives (UNRAE, Unione Nazionale Rappresentati Autoveicoli Esteri) was considered [27]. According to this assessment, passenger vehicles in Italy travel an average of 10,712 km/year, corresponding to approximately 30 km per day. Building on this outcome, two driving distances are considered: 30 km, representing a typical daily usage, and 120 km, accounting for scenarios involving longer trips.

As the analysis focuses on residential charging, electricity supply is assumed to occur through either a standard domestic socket (Schuko) or a wallbox. The aim of this paragraph is not to provide a comprehensive overview of charging technologies, but rather to clarify the power levels considered in the simulations. In Italy, one of the most common contractual power levels for residential users ranges between 1.5 kW and 3 kW; therefore, the domestic charge via a Schuko socket typically occurs at 2.3 kW. Conversely, wallbox solutions commonly operate at power levels of 3.7 kW and 7.4 kW [28]. Based on a market analysis, the 7.4 kW option is selected for the case study, [28]–[34]. **Table 1** summarizes the domestic charging configurations considered in this study.

Table 1. Characteristics of the chargers used

Charging option	Domestic socket	Wallbox
Rated charging power	2.3 kW	7.4 kW
Current type	AC	AC
Phase configuration	Single-phase	Single-phase

Type of Electric Vehicles

Currently, different types of EVs are available on the automotive market. Based on the degree of electrification, they are commonly gathered into four main categories. However, the section's aim is not to review the well-known characteristics, advantages, or drawbacks of each category of EVs, but rather to clarify the focus on BEVs from a charging perspective. These four categories are grouped into two broader classes according to the battery charging mechanism:

- The first class includes vehicles characterized by indirect battery charging. Mild Hybrid Electric Vehicles (MHEVs) and Full Hybrid Electric Vehicles (HEVs) do not allow direct charging through an external charging infrastructure. In MHEVs, battery

charging relies solely on regenerative braking, whereas in the second category, it is supported by both regenerative braking and the internal combustion engine.

- The second class involves vehicles enabling direct battery charging as PHEV and BEV. These vehicles can recharge their battery packs directly from the power grid through a charging point [21].

Building on these considerations, since the objective of this work is to optimize the battery charging schedule of vehicles to ensure a given driving range while minimizing the associated indirect CO_2 emissions, the analysis focuses exclusively on vehicles belonging to the direct battery charging category, specifically, the scope of the analysis is restricted to BEVs.

Once the vehicle category is defined, the next step involves assessing the national vehicle fleet to identify a representative passenger car for the case study. In 2024, the Italian vehicle fleet reached approximately 41.3 million units, with an average age of around 13 years. The fleet is still largely dominated by vehicles powered by traditional fuels: gasoline cars account for 42% of the total, followed by diesel vehicles at 40.9%. Regarding electric mobility, HEVs account for the largest share (6.8%), while PHEVs and BEVs together make up 0.7% of the total fleet [35]. The charging process analysis is carried out considering a representative compact BEV as a case study [36]. The selected vehicle belongs to the small city car segment and reflects one of the most widely adopted BEV configurations in the Italian passenger car market from 2021 to 2024, making it a representative choice for the domestic user segment [35]. The considered BEV is available with an electric motor rated at 45 or 65 hp and is equipped with a 26.8 kWh battery pack, which ensures a range of 225 km on a mixed cycle, including urban and extra-urban use, and 305 km on urban-only use. **Table 2** reports the main technical specifications, which are useful for contextualizing its dimensions and characteristics [37], [38].

Table 2. Main technical specifications of the selected BEV

Parameter	Value
Electric motor technology	Permanent magnet synchronous motor
Peak power	33 kW (45 hp)
Rated power	19 kW at 3000 rpm
Maximum torque	125 Nm at 500 rpm
Maximum speed	125 km/h
Acceleration (0 – 100 km/h)	19.1 s
Battery technology	Lithium-ion
Battery capacity	26.8 kWh
Energy consumption rate	<14.6 kWh/100 km
Curb weight	955 kg

Energy Performance of BEV

The energy consumption rate is a key parameter for BEVs, as it directly impacts the vehicle's range and, consequently, the distance that can be traveled. Usually, this data is reported by the manufacturer as results of the Worldwide Harmonised Light-Duty Vehicles Test Procedure (WLTP) cycle [39]. However, as discussed in the previous section, the actual energy consumption of electric vehicles depends on several factors. These factors can be grouped into three main categories: (i) driver related aspects, such as driving style and the use of auxiliary; (ii) external conditions related to the design of the city, the road, and traffic conditions; and (iii) weather conditions, in particular ambient air temperature [23], [40], [41]. Without real-world driving data or vehicle powertrain models, it is challenging to consider all these effects simultaneously. Therefore, this study focuses on the impact of air temperature on

the energy consumption factor of BEVs. The WLTP test is conducted at a reference temperature of 23 °C [42]. Several studies generally report that BEVs operate most efficiently within a temperature range of approximately 20 °C to 25 °C [22]. Deviations from this range, both at high and low temperatures, lead to increased energy consumption. This effect is mainly due to variations in the efficiency of power electronics components, changes in aerodynamic drag, rolling resistance, and the additional energy demand of thermal management and auxiliary systems. Although this has been widely demonstrated in the literature, low temperatures, in particular, have a greater impact on all these aspects, especially on the auxiliary system for thermal passenger comfort. Unlike internal combustion engine vehicles, BEVs cannot recover waste heat from the powertrain to heat the cabin. Instead, cabin heating relies on resistive heaters or heat pumps, which significantly increase electricity demand [23], [42], [43]. Although heat pumps improve energy efficiency compared to resistive heating, their performance still degrades as the air temperature drops [23], [42], [43]. Building upon these outcomes, the second step involves regression analysis to define a function that describes the relationships between outside air temperature and energy consumption. Obviously, a universal function applicable to all BEV models has not been developed, as this dependency is specific to each vehicle. The case study focuses on a specific vehicle model, and the required input data were retrieved from the range simulator available on the car manufacturer's website [25]. This tool enables the estimation of the selected BEV range based on the type of route, temperature, and vehicle settings. In this study, simulations were performed under urban driving conditions, with air conditioning activated and ECO modes deactivated. For each temperature value within the considered range, the estimated driving range was divided by the battery capacity to obtain the corresponding energy consumption factor. Table 3 reports the resulting dataset. Consistent with previous findings in the literature, temperature dependency exhibits different trends. Therefore, two distinct regression functions were carried out: one for temperatures below 20 °C and the other for those above 20 °C. In addition, continuity at the reference temperature was enforced by constraining both regressions to pass through the point (20 °C,12.8 kWh/100km).

Table 3. Input data for regression analysis

Temperature [°C]	Energy consumption factor [kWh/100km]
–5	18.5
0	17.3
5	15.8
10	14.9
15	14.1
20	12.8
25	13.4
30	13.4
35	13.7

Figure 3 shows the energy consumption factor of the selected BEV retrieved from the manufacturer's simulator; the dashed line represents the reference value of 14.6 kWh/100 km declared by the manufacturer. This highlights that for ambient temperatures above approximately 10 °C, the estimated energy consumption remains below the selected BEV reference value. Conversely, at lower temperatures, the consumption increases significantly and exceeds the manufacturer's declared value. For example, at –5 °C, the energy consumption factor reaches a value of 18.5 kWh/100 km, which is approximately 25% higher than the selected BEV reference value.

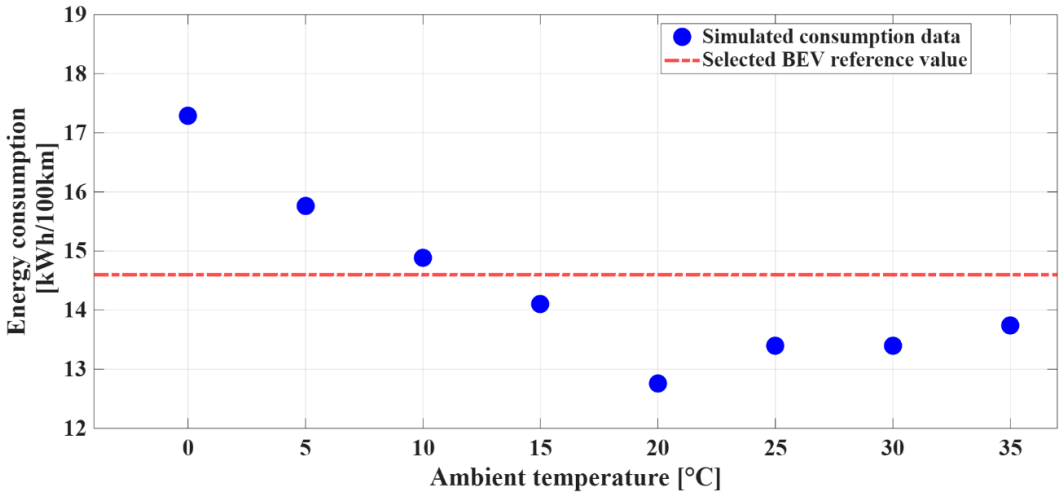

Figure 3. Energy consumption data retrieved from the manufacturer's simulator

CO_2 Emission Factors for the Italian Power Grid

As mentioned previously, the CO_2 emission factor of the Italian electricity system used in this work is derived from national electricity production data. Since the case study focuses on 2023, it is necessary to provide an overview of the national electricity generation mix for that year. In this context, the statistical report published by Terna, the Italian Transmission System Operator (TSO), represents a reliable source, as it provides a detailed breakdown of electricity production by primary energy source [44]. An analysis of the 2023 electricity mix reveals a decrease in electricity generation from thermoelectric power plants compared to 2022, which nonetheless still accounted for approximately 58% of total national production. Conversely, electricity generation from RESs increased by 16% compared to 2022, reaching a share of 37.1% of gross domestic electricity consumption, net of pumping contributions. A more detailed analysis of production from RESs in 2023 shows a strong recovery in hydroelectric generation, which increased by 42.7% compared to 2022 levels, reaching approximately 40 TWh, thus confirming hydropower as the main RES in the national energy mix. Wind power generation also recorded a significant increase, reaching 23.6 TWh, while photovoltaic production set a new record, at 30.7 TWh. In contrast, electricity generation from bioenergy declined by 9.1%, resulting in a decrease of 16 TWh. Moreover, for the fourth consecutive year, electricity production from geothermal sources continued to decline, settling at 5.7 TWh. **Figure 4** shows the percentage contribution of the different energy sources to national electricity production in Italy in 2023.

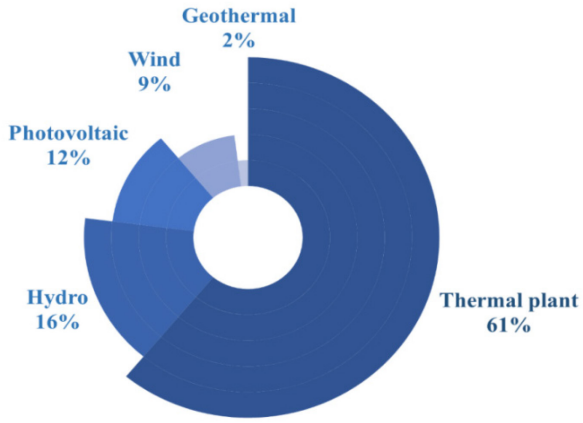

Figure 4. Percentage contribution of different energy sources to Italian electricity production in Italy in 2023 – TERNA

By cross-referencing these aggregated national data with the hourly electricity production profiles of all power plants, obtained from the Transparency Platform of ENTSO-E (European Network of Transmission System Operators for Electricity), the national electricity mix was reconstructed at an hourly resolution [45]. Subsequently, ISPRA (Istituto Superiore per la Protezione e la Ricerca Ambientale, The Italian Institute for Environmental Protection and Research) provided technology-specific CO_2 emission factors for electricity production in 2023, differentiated by primary source [46]. Based on these data, total CO_2 emissions associated with electricity generation were calculated for each hour of the year. Knowing the amount of CO_2 emitted as a result of electricity production from thermoelectric plants, three scenarios were defined. For the first emission factor, $\alpha_{\mathrm{TE_F}}$, only thermoelectric plants powered by fossil fuels were considered. The second factor, $\alpha_{\mathrm{TE_{F+B}}}$, includes thermoelectric plants fueled by both fossil fuels and biofuels. Finally, the third emissions factor, $\alpha_{\mathrm{TE_{F+RES}}}$, accounts for total electricity production, including both fossil-based and renewable sources. By definition, $\alpha_{\mathrm{TE_{F+RES}}}$ represents CO_2 emissions per unit of electricity withdrawn from the grid and therefore reflects, on an hourly basis, the actual national electricity production mix. More details of the methodology adopted are reported in [19]. In the case study, the additional electrical load associated with the BEV charging was assumed to be sufficiently small so as not to significantly alter the national electricity production mix. Therefore, the CO_2 emissions factor α_{TE_F+RES} was adopted for the assessment of indirect CO_2 emissions.

Figure 5 shows the values of the emission factor $\alpha_{\mathrm{TE_{F+RES}}}$, calculated at daily and hourly resolution for the whole of 2023. The *y*-axis reports the emission factor values, the x-axis represents the days of the year, and the colour scale, ranging from blue to red, represents the hour of the day. An analysis of the trend reveals higher average values in the winter months and lower average values during the summer months. This seasonal behavior can be mainly attributed to the increased contribution of renewable sources in the summer months, particularly photovoltaic generation, which benefits from higher solar irradiance. Figure 5 also shows that, for the same season and day, the highest emission factor values are consistently associated with the early morning and nighttime hours, whereas the lowest values occur during the midday hours. Specifically, maximum values of $\alpha_{\mathrm{TE_{F+RES}}}$ are recorded in the time slot from approximately 0:00 AM to 4:00 AM (blue dots) and after 8:00 PM (red dots), while the minimum values are recorded between approximately 9:00 AM and 4:00 PM. This intraday variability is again attributable to the higher penetration of renewable generation, especially photovoltaic production, during daylight hours.

For the purposes of this work, the hourly values of the emission factor were converted to a 15-minute time resolution in order to ensure consistency with the temporal resolution adopted for the charging schedule. Each hourly emission factor was assumed to be constant over the corresponding four 15-minute intervals.

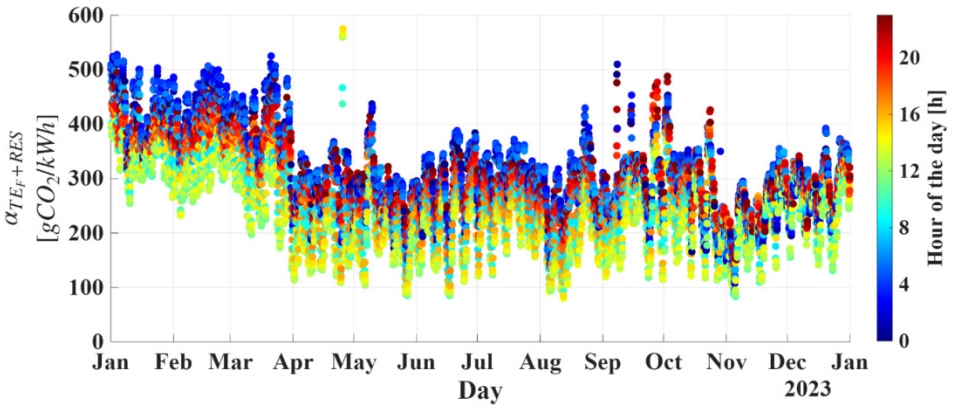

Figure 5. Trend of CO2 emissions factor α_(TE_(F+RES)) for 2023

In case of large-scale EV adoption, the use of marginal CO_2 emissions factors would be more appropriate, since a substantial increase in electricity demand does not translate into a proportional change in the output of all generating units [47]. Indeed, only a limited subset of power plants can ensure the required operational flexibility and rapid response to load variations, and these units typically determine the marginal CO_2 emissions of the power grid rather than the overall production mix.

Marginal emissions factors can be calculated either ex ante by solving an optimal dispatch problem within an energy model of the electricity system, or ex post by analysing electricity market data or production data. In the latter case, marginal emissions can be inferred through the merit order principle, which links marginal emissions to marginal technology, or through regression-based approaches that quantify the relationship between variations in electricity production and associated CO_2 emissions [17]. While these approaches are well established in the literature, their application would shift the focus of the present study from an emission-aware charging strategy at the individual user level to a system-level assessment of electricity generation dispatch. Since the additional load associated with a single BEV is assumed not to significantly affect the national generation mix, the analysis uses hourly-average grid emission factors. A comprehensive treatment of marginal emission factors and their computation is therefore beyond the scope of this work.

Finally, the hourly unit electricity prices (PUN) for the year 2023 were retrieved from the platform made available by the Italian electricity market operator (GME) [48]. These data were cross-referenced with the percentage share of renewable energy sources in the national electricity production mix, previously calculated. The resulting relationship is illustrated in Figure 6. The *y*-axis reports the hourly electricity price, while the *x*-axis represents the days of the year. The colour scale, ranging from blue to red, indicates the share of renewable generation in the production mix. It can be observed that periods characterised by higher renewable penetration (red markers) generally correspond to lower electricity price levels. This evidence supports the argument that emission-based and price-based charging strategies are not necessarily conflicting approaches, but may instead exhibit complementary dynamics under typical market conditions.

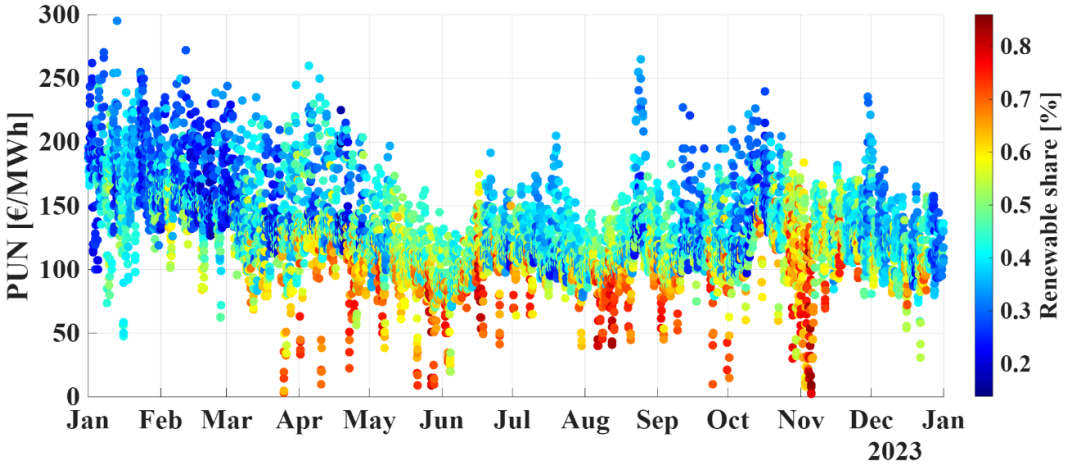

Figure 6. Relationship between hourly electricity prices and renewable generation share in the Italian electricity mix for 2023

V1G$_{CO2}$ Optimization Algorithm

This section describes the core of the algorithm implemented for defining an environmentally driven smart BEV charging strategy, V1G$_{CO2}$. The optimization framework aims to determine a daily charging schedule, $sched_{d}^{r,P}$, for each distance r and rated power charging P, that minimizes indirect CO_2 emissions associated with electricity consumption,

while ensuring the energy required to meet a predefined driving range. The procedure began with the evaluation of the average daily air temperatures for the city of Benevento over the time interval from 6:00 AM to 7:00 PM. The average temperature, denoted as T_d, is computed for each day d of the year. Based on T_d, the second step of the algorithm consists of calculating the daily energy needed, E_d^r, to cover a given range, r, for each day of 2023, as shown in the following equation:

$$E_d^r = e_c(T_d) \times r \quad (1)$$

where $e_c(T_d)$ represents the energy consumption factor of BEV obtained from the regressions assessment, described in Section 2.2.1, as a function of mean outdoor air temperature.

Once the daily energy demand is defined, the charging window is defined with a temporal resolution of fifteen minutes, between 8:00 PM on day d and 5:00 AM on day d+1. For each time slot within this interval, the corresponding emission factor $\alpha_{TE_{F+RES}}$ is identified. The time slots are then sorted in ascending order according to their associated emission factor values, so that the first elements of the ordered set correspond to the periods with the lowest carbon emissions. The allocation of the energy to be recharged (E_d^r) is performed to be equal to the energy consumed during the day. For each fifteen-minute time slot in the sorted list, the algorithm assigns an amount of energy equal to the minimum between the maximum energy that can be drawn from the grid, depending on the selected charging power, and the residual energy still to be recharged. After each allocation step, the residual energy demand is updated, and the procedure continues until either the required energy is fully recharged or the charging window is exhausted. This iterative process yields a daily recharging schedule that prioritizes low-emission time slots and is tailored to each combination of driving distance and charging power.

Furthermore, it is important to emphasize that the optimization algorithm is explicitly designed to ensure that the BEV is fully charged and ready for use at the predefined departure time, even when the charging process is temporally shifted within the available charging window. The only circumstance under which the vehicle would not reach full charge by 5:00 AM is not related to the charging strategy itself, but rather to physical constraints of the charging process. Specifically, if the total energy required exceeds the energy that can be delivered within the available charging window, given the available charging power, full recharging cannot be achieved regardless of the scheduling strategy adopted.

Before the charging process starts and after each charging step, the battery's State Of Charge (SOC) is evaluated to verify whether the available charging window is sufficient to meet the energy demand. According to recent literature, maintaining the SOC within the range of 20% - 80% is recommended to preserve battery health and limit degradation phenomena, as a series of deep discharges can compromise the battery's functionality **[49]**, **[50]**. In line with these findings, an initial SOC value of 80% is assumed in the case under study. With this aim, the residual energy stored in the battery at the end of the day driving, $Q_{residual,d}^r$ is calculated as shown in the following equation:

$$Q_{residual,d}^r = Q_{max} \times SOC_{in} - E_d^r \quad (2)$$

where: Q_{max} is the battery capacity of the selected BEV, as reported in **Table 2**; SOC_{in} is the initial charge level, 80%; and E_d^r is the energy required to travel a distance r on the day d. The SOC at the end of the driving phase is then calculated as stated by the equation:

$$SOC_d^r = \frac{Q_{residual,d}^r}{Q_{max}} \times 100 \quad (3)$$

During the charging phase, the residual energy stored in the battery is dynamically updated by adding the energy allocated at each time step. Although SOC can be used to modulate charging power in advanced charging strategies in order to preserve the battery's useful life, in this work, the charging process is assumed to occur at constant power, without the implementation of SOC-dependent charging strategies [49].

It is also worth noting that potential issues related to battery degradation are not addressed in this study. Battery degradation phenomena are widely documented in the literature and are commonly classified into calendar ageing and cycle ageing, the latter being directly influenced by charging conditions. In particular, battery ageing is known to depend on several factors, including the charging and discharging C-rate, the SOC level, and the ambient temperature at which charging occurs [51]. Although degradation effects are unavoidable in practice, their impact is expected to be limited under the operating conditions considered in this work. Indeed, several studies report that prolonged charging at high C-rates can accelerate battery ageing, an effect that is further exacerbated when high C-rates are combined with high SOC levels [51]. In the present study, the maximum SOC after charging is capped at 80%, a commonly recommended threshold to preserve battery health. Moreover, the charging process is characterised by low C-rates. For the two charging power levels considered (2.3 kW and 7.4 kW), the corresponding C-rates are approximately 0.09C and 0.27C, respectively (computed as the ratio of charging power to the battery's nominal capacity), i.e., well below 1C. Previous studies indicate that slow AC charging at low C-rates is generally associated with slower degradation processes [51] and higher energy efficiency compared to high-power charging [52].

If battery degradation were explicitly included in the analysis, it would mainly manifest as a gradual reduction in the usable battery capacity over time. From a modelling perspective, this would translate into higher energy demand for the same driving distance and outdoor temperature, resulting in lower SOC at the end of the driving phase. However, the structure of the proposed charging optimisation algorithm would remain unchanged, as it is formulated to allocate the required charging energy within the available charging window, independently of the underlying causes of capacity reduction.

CO_2 Emissions Calculation and Baseline Scenario

The developed algorithm enables the calculation of CO_2 emissions associated with BEV charging for each combination of day *d*, travelled distance *r*, and charging power *P*. The daily CO_2 emission, $CO_{2,d}^{r,P}$ are calculated as shown in the following equation:

$$\mathrm{CO}_{2,\mathrm{d}}^{\mathrm{r,P}} = \sum_{i=h_{\mathrm{start}}}^{h_{\mathrm{end}}} sched_{\mathrm{d}}^{\mathrm{r,P}}\ (i) \times \alpha_{\mathrm{TE_{F+RES_d}}}(i) \tag{4}$$

where h_{start} and h_{end} denote the beginning and the end of the charging window, respectively; $sched_{\mathrm{d}}^{\mathrm{r,P}}(i)$ represents the energy charged during the *i*-th 15-minute time slot; and $\alpha_{\mathrm{TE_{F+RES_d}}}(i)$ is the corresponding carbon emission factor of the Italian power grid at the same time step.

RESULTS

This Section presents and discusses the results obtained from implementing the proposed optimization algorithm, developed in the MATLAB environment.

Regression Assessment

As shown in **Table 3**, the temperature data used as input for the regression analysis span a wide range, from –5 °C to 35 °C. Therefore, before proceeding with the regression analysis, the average daily temperatures were calculated, as described in Section 2.1. **Figure 7** shows the resulting temperature profile for the city of Benevento over the reference year. The graph supports the consistency of the adopted regression approach, as it clearly shows that the air temperature range considered in the regression, highlighted by the lower and upper bounds with dashed red lines, encompasses all the average daily temperatures calculated for Benevento.

Based on the analysis of average daily temperatures, it can be inferred that the EV operates predominantly under non-optimal climatic conditions. During the winter, the average temperature frequently falls below 10 °C, with minimum values reaching approximately 1.8 °C. In contrast, during summer, it often exceeds 30 °C, with peak values close to 35 °C. As discussed in Section 2.2.1, both low and high temperatures negatively impact the energy efficiency of BEVs, underscoring the importance of explicitly accounting for temperature effects in estimating energy consumption.

Figure 8 shows the regression functions developed in the MATLAB environment, while **Table 4** reports the coefficients of the regression functions. These two functions describe the relationship between the energy consumption factor of the selected EV and the outside temperature, representing a key input to the entire optimization framework. The analysis of the figure reveals two distinct behaviors, depending on whether the temperature is lower or higher than the reference value of 20 °C. This change in trend confirms the need to adopt two separate regression functions to accurately represent the temperature-dependent variation of the consumption factor.

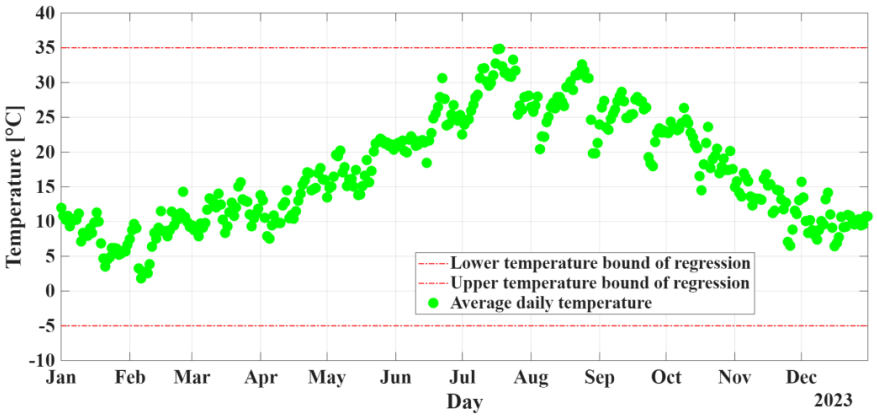

Figure 7. Average daily temperatures for Benevento

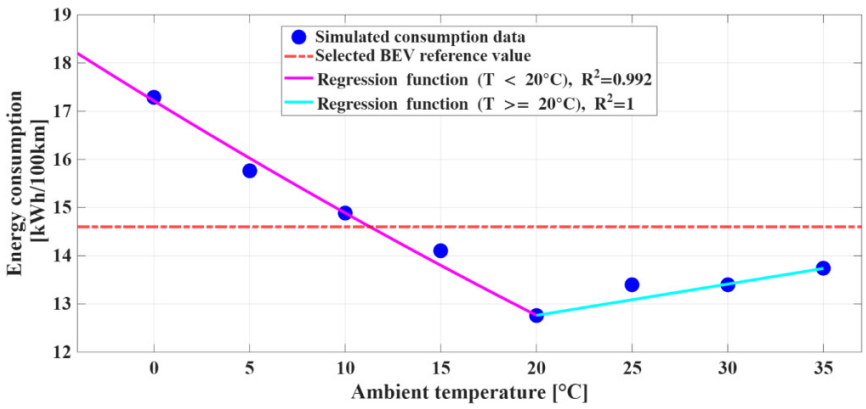

Figure 8. Regression energy consumption factor outcomes as function of ambient temperature

Table 4. Regression functions outcomes

Energy consumption function for temperature < 20 °C		
$e_c(T) = aT^2 + bT + c$		
$a = 0.001013$	$b = -0.2428$	$c = 17.21$
Energy consumption function for temperature ≥ 20 °C		
$e_c(T) = dT + e$		
$d = 0.06494$		$e = 11.46$

Energy Performance of BEV

The results of the analysis on the energy performance of BEVs are presented below, with the aim of highlighting the influence of temperature on the energy consumption factor of BEVs. In this context, the consumption factor of the selected BEV was calculated for each day of 2023 by applying the two previously developed regression functions and the average daily temperatures for Benevento during vehicle operating hours.

The results are summarized in **Figure 9**, which illustrates the trend in the energy consumption factor throughout 2023. A colour scale is adopted to represent the corresponding average daily temperature, ranging from dark blue (low temperatures) to dark red (high temperatures). The figure clearly shows higher energy consumption factors during the winter months due to the strong impact of low temperatures; conversely, lower values are observed during the summer and mid-season periods.

The lowest temperatures occur at the beginning of February, as indicated by the dark blue markers, for which the corresponding energy consumption factor values are the highest. The maximum value reaches 16.8 kWh/100 km. During the summer months, although temperatures reach around 30 °C – 35 °C, the energy consumption factor remains lower and consistently below the reference threshold value of 14.6 kWh/100 km. The energy consumption factor reaches the minimum value of 12.8 kWh/100 km at an average air temperature of 20 °C. Overall, the results indicated that, when considering temperature effects alone, among the various factors affecting the car's performance, the vehicle performs less efficiently than the manufacturer's stated figures when the temperature drops below 10°C.

Table 5 reports the minimum, maximum, and average values for both temperature and energy consumption factor. Despite the presence of extreme values, the annual average energy consumption factor is 14 kWh/100 km, which remains lower than the reference threshold value.

The analysis of the results related to the electrical energy required by the vehicle to travel a certain distance further confirms the strong dependence of BEV energy performance on temperature. The results show that the energy demand on the electrochemical storage system during the summer months is significantly lower than that observed in winter. In fact, the maximum value, equal to 5.03 kWh, occurs on February 6th, while the minimum, 3.83 kWh, occurs on May 22nd. The corresponding annual average value is 4.19 kWh.

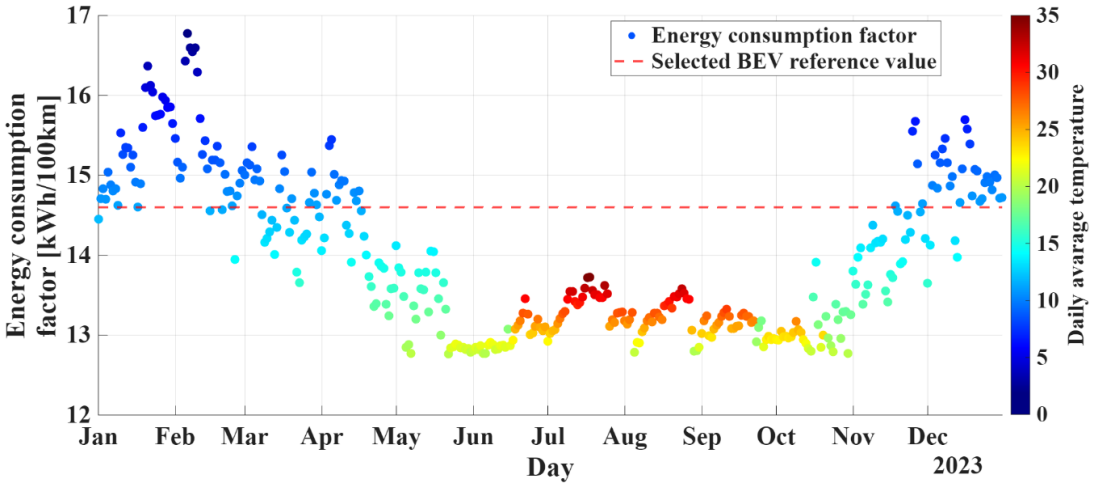

Figure 9. Energy consumption trends for BEV over the reference year

Table 5. Minimum, maximum, and average values for temperature and energy consumption factor

Daily average temperature [°C]		
min	max	mean
1.8	34.9	17.3
Energy consumption factor [kWh/100 km]		
min	max	mean
12.8	16.8	14.0

A similar trend is observed for the distance of 120 km. In this case, the minimum value, equal to 15.32 kWh, and the maximum value, 20.13 kWh, occur on the same day identified for the 30 km scenario, while the annual average energy demand amounts to 16.76 kWh. This behavior is primarily attributable to the impact of temperature on BEV energy consumption, which becomes particularly pronounced under cold climatic conditions.

Consequently, low-temperature conditions lead to a disproportionate increase in energy demand compared to high-temperature conditions. This behavior is not specific to the selected BEV but is consistent with findings widely reported in the literature for BEV.

The monthly analysis further corroborates the daily results, showing higher energy demand during the winter months compared to the summer period, as shown in **Figure 10**.

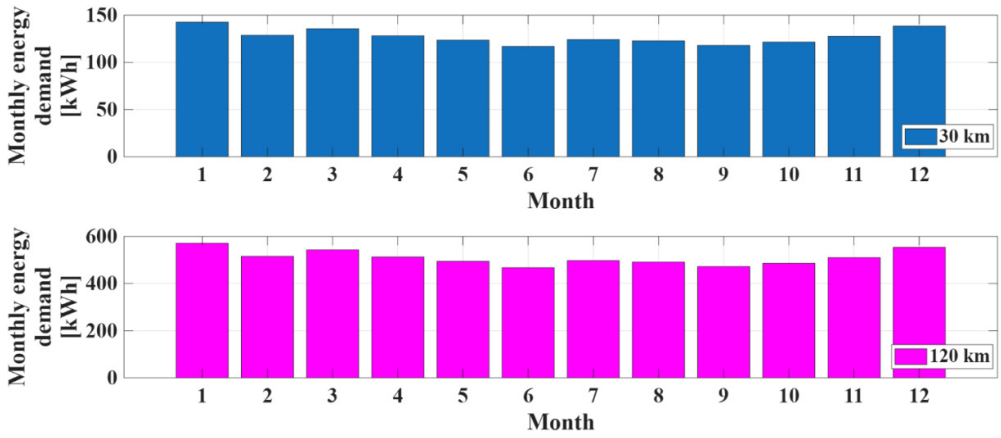

Figure 10. Monthly energy demand

In addition, the algorithm developed in MATLAB also calculates the SOC of the selected BEV at the end of each daily trip throughout 2023. **Figure 11** shows the daily SOC values as a

function of the travelled distance. A red dashed line indicates the 20% SOC threshold, below which it is advisable not to fall in order to preserve the vehicle's battery life and efficiency. The figure shows that, even in the most critical months (winter), the SOC remains above the threshold for short daily distances (30 km). Conversely, for longer distances (120 km), range-related issues begin to arise. Furthermore, for short distances, the influence of the ambient temperature appears to be limited: the SOC never falls below 60% and generally remains close to 65% throughout the years. In the case of longer distances, however, the effects of temperature are more noticeable, resulting in significant SOC variability. For instance, in February, the SOC range spans from a minimum value of 4.9%, recorded on February 5th, to a maximum value of 17.6%, observed on February 25th.

These results highlight potentially critical operating scenarios for BEVs, particularly during winter. From a battery preservation perspective, adopting intermediate charging events instead of a single end-of-day recharge could be a viable mitigation measure to avoid prolonged periods at low SOC levels. This consideration does not stem from the environmentally driven charging strategy itself, but rather from the harsh climatic conditions that exacerbate energy consumption and lead to deeper discharge cycles during vehicle operation.

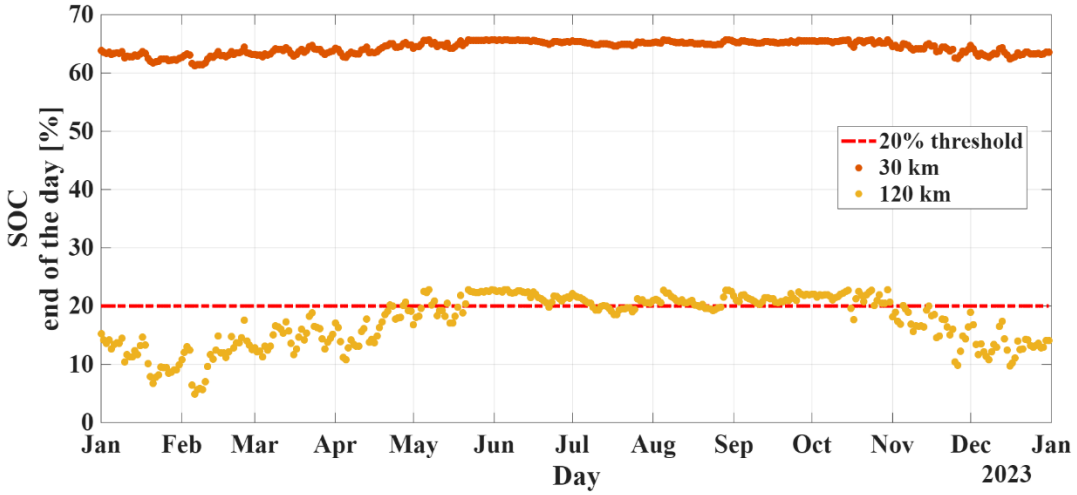

Figure 11. SOC at the end of the day for each day of the reference year

Charging Optimization Results

Initially, the average charging times were calculated for the two charging powers considered, along with the corresponding travelled distances. The results, expressed in hours, are reported in **Table 6**. Overall, the average charging duration ranges from approximately 35 minutes to more than 7 hours, depending on the combination of distance travelled and charging power. For the purposes of this study, and to facilitate the interpretation of the optimization results, charging events are grouped into two categories: short charging sessions, with durations shorter than 2 hours (typically associated with short distances or high charging power), and long charging sessions, with durations exceeding 5 hours (associated with long distances or low charging power). This distinction is particularly relevant for the subsequent analysis of charging optimization strategies and their interaction with time-varying grid emission factors.

Table 6. Average charging time [h] as a function of travelled distance and rated charging power

Rated charging power [kW]	Distance [km]	
	30	120
2.3	1.8	7.3
7.4	0.6	2.3

Charging schedule optimization. Continuing the analysis of the results, this subsection presents the charging schedules obtained by applying the $V1G_{CO2}$ optimization algorithm under different operating conditions.

Figure 12 shows the histogram of charging start times, highlighting their temporal distribution with respect to the electricity grid emission factor considered. A clear peak is observed at 8:00 PM, indicating a high frequency of charging initiations at this time. The results, therefore, suggest that, from an environmental perspective, it is preferable to start charging at 8:00 PM and avoid prolonging the charging period until midnight. Analyzing these results in relation to the uncontrolled charging (baseline scenario) reveals that it has a less environmental impact only in cases of short charging durations. In such situations, charging is mainly concentrated between 8:00 PM and 9:00 PM, when emission factors are at their minimum.

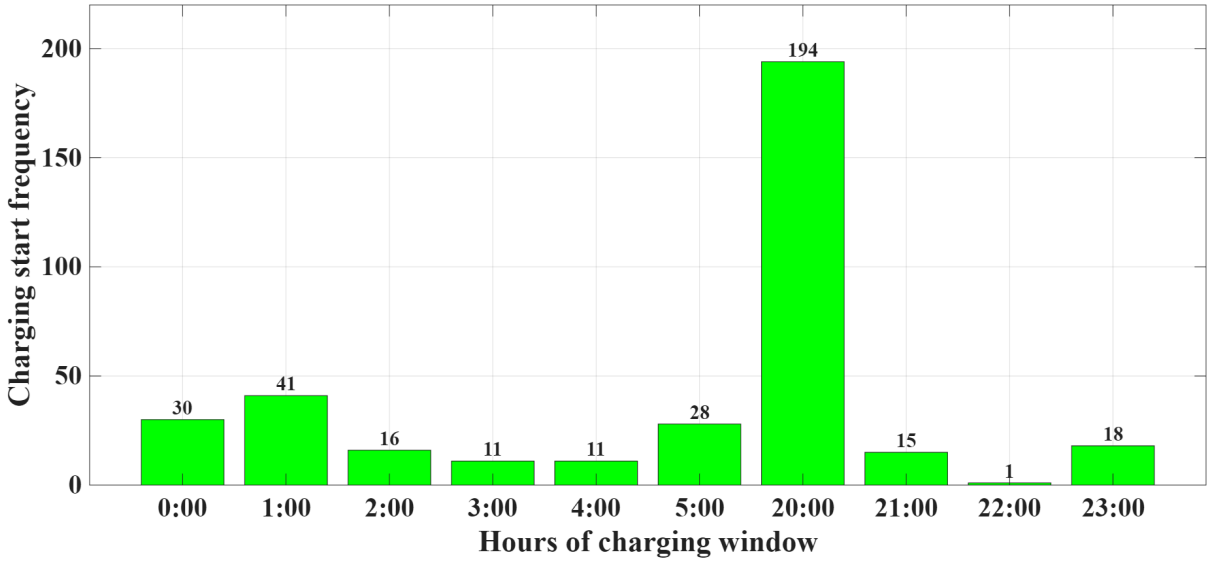

Figure 12. Frequency relative to charging start hours

The following results illustrate the charging schedules obtained according to the $V1G_{CO2}$ logic for a representative day, 15 January, in the city of Benevento. This specific day was chosen because it presents conditions that clearly illustrate the result of the optimization process implemented. On this day, the average daily temperature is 8.4 °C, corresponding to an energy consumption factor of 15.3 kWh/100 km. Consequently, the energy demand to travel 30 km and 120 km is equal to 4.6 kWh and 18.3 kWh, respectively.

Figure 13 shows the results of the optimization algorithm for a charging power of 2.3 kW and a distance traveled of 30 km. The primary y-axis displays the distribution of energy across the various 15-minute time slots, while the secondary y-axis represents the corresponding quarter-hourly trend of the grid emission factor. The first step taken by the algorithm is to identify the time slots characterized by the lowest emission factor. In this case, the interval between 1:00 AM and 2:00 AM exhibits the minimum values, with approximately 92 gCO_2 emitted per quarter of an hour.

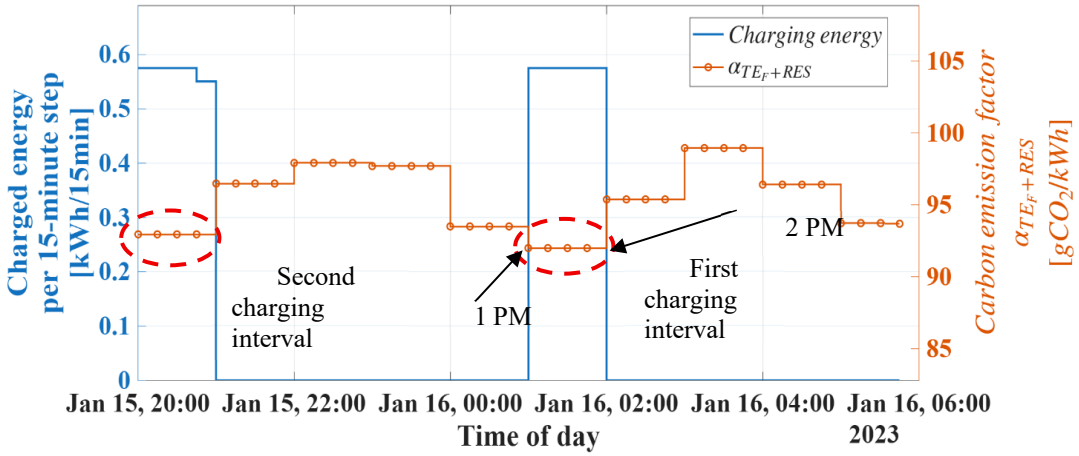

Figure 13. Charging schedule for rate charging power 2.3 kW and traveled distance of 30 km – 15 January

The algorithm, therefore, allocates the rechargeable energy to these four time slots. Since the energy required is not fully satisfied at the end of this interval, the algorithm subsequently selects the second most favourable time window, between 8:00 PM and 9:00 PM, during which the emission factor is approximately 93 gCO_2 per quarter of an hour. The algorithm allocates the maximum rechargeable energy, 0.58 kWh, in the first three slots, while the remaining energy (0.55 kWh) is allocated in the last slot.

It should be noted that, since the quarter-hourly emission factors of the electricity grid are derived from hourly values, the charging occurs in consecutive 15-minute intervals. With the update of the methodology for calculating the emission factors of the electricity grid, which is now based on a 15-minute interval rather than an hourly basis, charging schedules could become more fragmented and potentially even more optimized.

For comparison under uncontrolled charging conditions, charging would have occurred continuously between 8:00 PM and 10:00 PM, thus including time intervals associated with relatively high emission factor values.

Figure 14 presents the results of the optimization algorithm for a charging power of 2.3 kW and a travelled distance of 120 km, a case representative of long charging durations. This scenario is particularly informative, as it highlights the limitations of the optimization algorithm when the required charging time exceeds a significant portion of the available charging window. In this case, more than 7 hours of charging are required out of the 10 hours available. As a result, although the algorithm prioritizes low-emission time slots, it can only avoid allocating energy during the two most emission-intensive intervals: from 10:00 PM to 11:00 PM and from 3:00 AM to 4:00 AM, characterized by approximately 97 gCO_2 and 98 gCO_2 per quarter of an hour, respectively.

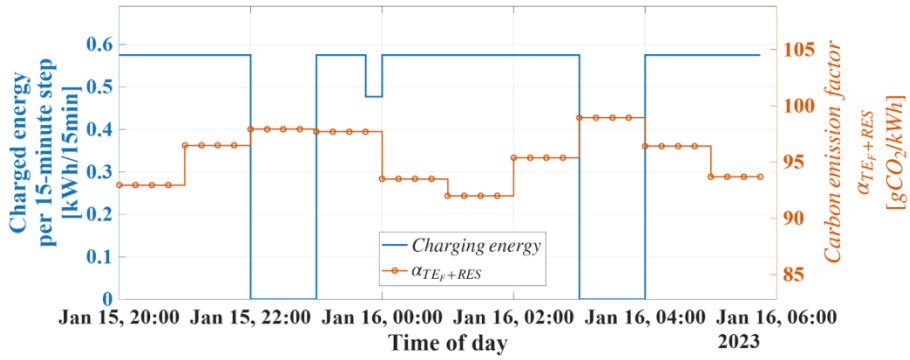

Figure 14. Charging schedule and SOC evolution for rate charging power 2.3 kW and traveled distance of 120 km - 15 January

Figure 15 reports the case of a short charging session with a rated charging power of 7.4 kW and a travelled distance of 30 km. Since the total charging duration is approximately 36 minutes, the algorithm allocates the rechargeable energy entirely in the lowest-emission time slot. This scenario clearly demonstrates that in the case of short charging sessions, the V1G$_{CO2}$ algorithm is particularly effective in minimizing the indirect CO_2 emissions associated with BEV charging.

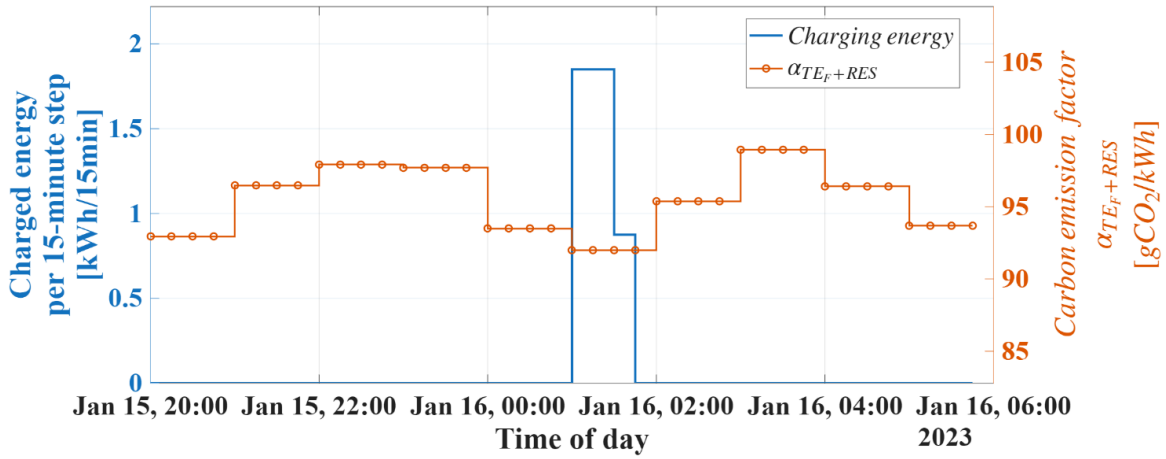

Figure 15. Charging schedule and SOC evolution for rate charging power 7.4 kW and traveled distance of 30 km – 15 January

Indirect CO_2 emission associated with BEV charging. To evaluate the effectiveness of the proposed optimization algorithm, the daily and annual indirect CO_2 emissions associated with the BEV charging process were calculated for each scenario. **Figure 16** reports the daily CO_2 emissions obtained for a rated charging power of 7.4 kW and a travelled distance of 120 km. The results clearly show higher emission levels during the winter months compared to the summer period. The maximum daily emission, equal to 2036 gCO_2, was recorded on January 23rd, whereas the minimum value of 412 gCO_2 occurred on November 4th. The corresponding annual average value is 997 gCO_2 per day. This seasonal trend can be explained by the combined effect of two main factors: the energy consumption factor of EVs is higher during winter months due to lower ambient temperatures, and the electricity grid emission factors are generally higher in winter, reflecting a reduced contribution from RESs.

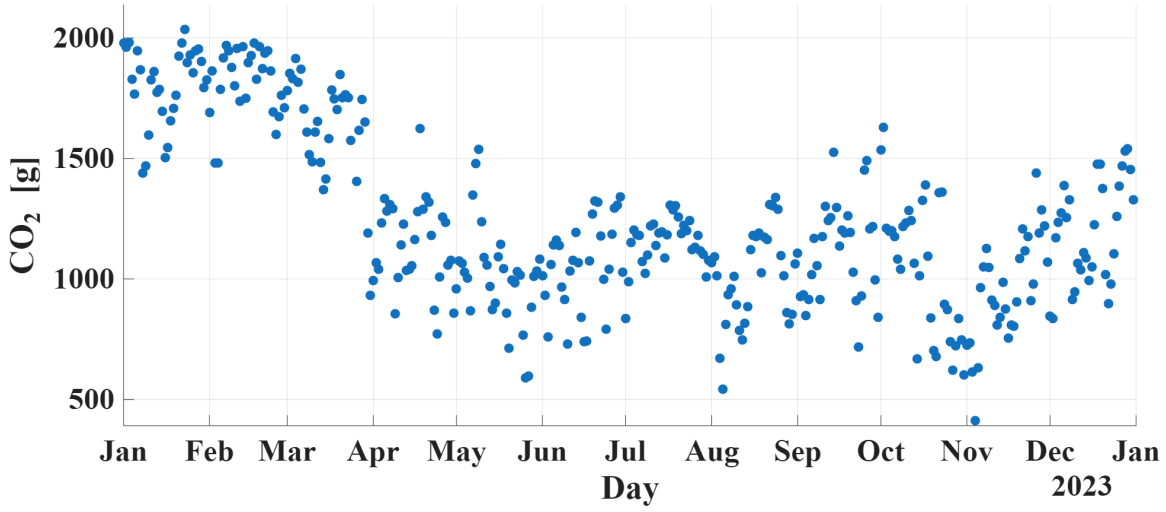

Figure 16. Daily indirect CO2 emissions – travelled distances 120 km, rated power charging 7.4 kW

For the sake of brevity, the corresponding daily emission profiles for the other scenarios are not reported, as they exhibit analogous trends. A comprehensive overview of the annual indirect CO_2 emissions is provided in **Table 7**, which summarizes the total annual emissions as a function of travelled distance and charging power.

Table 7. Annual indirect CO2 emissions [kgCO2/year]

Rated charging power	Distances	
	30 km	120 km
2.3 kW	112	478
7.4 kW	111	452

A further key indicator for assessing the environmental performance of EVs is the average annual values of specific CO_2 emissions, expressed per unit distance travelled. **Table 8** reports the values obtained in the different scenarios. For short travelled distances, corresponding to short charging sessions, the influence of charging power is negligible: the specific emissions range from 10.1 gCO_2/km to 10.3 gCO_2/km for charging powers of 7.4 kW and 2.3 kW, respectively. This result is explained by the structure of the optimization algorithm, which concentrates charging in time intervals characterized by the lowest emission factors. In contrast, for long travelled distances, and therefore long charging durations, the charging power plays a more significant role. In this case, the maximum specific emissions value of 10.9 gCO_2/km, observed at low charging power, decreases to 10.3 gCO_2/km when a higher charging power is adopted. These results further confirm that the effectiveness of the $V1G_{CO2}$ strategy increases as the flexibility in allocating charging energy across low-emission time slots improves.

Table 8. Average annual values of specific CO2 emissions [gCO2/km]

Rated charging power	Distances	
	30 km	120 km
2.3 kW	10.3	10.9
7.4 kW	10.1	10.3

Uncontrolled Charging Strategy

To assess the potential environmental benefits of the proposed $V1G_{CO2}$, the CO_2 emissions associated with the optimized BEV charging strategy are compared with those obtained under uncontrolled charging. **Table 9** reports the annual CO_2 emissions for all the analyzed scenarios. The comparison clearly shows that, in all scenarios, uncontrolled charging leads to an increase in CO_2 emissions. Annual emissions range from 117 $kgCO_2$ in the case of short charging sessions to 489 $kgCO_2$ for long charging sessions. In the case of short recharges, corresponding to a travelled distance of 30 km, the adoption of the $V1G_{CO2}$ strategy leads to an annual emission reduction of approximately 5% – 6%; while in the case of long recharges, as discussed previously, the effectiveness of the optimization decreases, with emission reductions limited to around 2%. This behavior is consistent with the reduced flexibility in allocating charging energy when a large fraction of the available charging window is required.

To correctly interpret the relatively modest reductions observed even in the most favourable scenarios, it is important to note that the effectiveness of the optimization algorithm depends not only on the duration of the charging process but also on the temporal position of the minimum grid emission. On days when the minimum coincides with the beginning of the charging window (8:00 PM), the optimization yields limited additional benefits, as uncontrolled charging naturally occurs during low-emission time slots. **Figure 12**, with reference to the α_{TE_F+RES} parameter, shows that, over the year, the minimum emission factor

occurs at 8:00 PM on 194 days; therefore, in more than half of the year, the minimum coincides with user-driven charging. Nevertheless, in the remaining cases, when the minimum emissions factor occurs later in the night, the optimization algorithm effectively shifts charging away from periods with higher emissions, leading to measurable CO_2 reductions.

Table 9. Annual indirect CO2 emissions [kgCO2/year] – uncontrolled charging strategy

Rated charging power	Distances	
	30 km	120 km
2.3 kW	119	489
7.4 kW	117	478

These results highlight that the $V1G_{CO2}$ strategy is particularly effective when sufficient temporal flexibility exists and when low-emission electricity is available outside the natural user-driven charging start time. Consequently, the proposed approach demonstrates its greatest potential in scenarios characterized by higher variability in the electricity mix and longer charging windows.

Finally, it is important to note that these results refer to charging a single BEV. However, if a fully electrified Italian passenger vehicle fleet is assumed, the proposed strategy would lead to an annual reduction in 2023 of approximately 4766 $ktCO_2$/year, while preventing a potential increase of about 7% in total passenger transport sector emissions that would otherwise occur in the absence of charging optimization.

CONCLUSIONS

This study investigated the optimization of BEV charging with the goal of reducing indirect CO_2 emissions through a controlled V1G charging strategy. Unlike conventional approaches based on grid-oriented signals, such as those related to ancillary services or grid stability, the proposed $V1G_{CO2}$ strategy is driven by an environmental signal, namely the time-varying CO_2 emission factor of the grid electricity.

The analysis focused on a representative and widely adopted BEV model in the Italian context, considering domestic users charging after working hours (from 8:00 PM to 6:00 AM) using either a standard domestic socket (2.3 kW) or a wallbox (7.4 kW). Two daily distances, 30 km and 120 km, were considered to represent short and long charging sessions, respectively. The city of Benevento was selected as a case study, and the analysis was carried out for the entire year 2023.

A key contribution of this work lies in the explicit modeling of the variability in BEV energy performance as a function of outside temperature. Using manufacturer-provided data, two regression functions were developed to describe the temperature-dependent energy consumption factor of the vehicle. The results highlight a pronounced seasonal variability, with significantly higher consumption values during winter months. This effect becomes particularly critical for long daily distances, for which the SOC may approach or fall below recommended thresholds under unfavorable thermal conditions. Accurately representing this dependency is essential to realistically estimate both energy demand and associated emissions.

A second major contribution concerns the treatment of electricity grid emissions factors. Rather than assuming constant or average values, this study reconstructed time-varying CO_2 emission factors for the Italian power system based on the actual national electricity mix in 2023. The resulting hourly and subsequently 15-minute profiles reveal strong temporal variability, with systematically lower emission factors during daytime hours and higher values during evening and nighttime periods. This finding confirms that post-work charging generally occurs in a non-optimal environmental time window, thereby motivating the need for controlled charging strategies.

Building on these elements, a MATLAB-based optimization algorithm was developed to allocate BEV charging energy within the available charging window by prioritizing time slots characterized by lower emission factors. The algorithm operates at 15-minute resolution and computes the indirect CO_2 emissions associated with each charging session. A baseline scenario of uncontrolled charging, in which energy is drawn immediately upon arrival without an optimization logic, was also defined to enable a direct comparison.

The results clearly demonstrate that controlled charging systematically outperforms uncontrolled charging in terms of CO_2 emissions. For short daily distances (30 km), annual emissions are approximately 100 $kgCO_2$, with negligible differences between charging powers. In this case, the optimized strategy achieves emission reductions of up to 5.7% compared to the baseline scenario. For longer distances (120 km), annual emissions increase to approximately 400-500 $kgCO_2$; although the absolute benefits of optimization are reduced, lower charging power still allows for emission reductions of around 2-3%.

A crucial outcome of this study is the demonstration that BEV charging flexibility is effectively exploitable only in the case of short charging sessions. When charging durations are limited, the algorithm can concentrate energy withdrawal in low-emission time slots, maximizing environmental benefits. Conversely, for long charging sessions, the need to occupy a large fraction of the available charging window inevitably leads to the inclusion of less favourable periods, reducing the effectiveness of optimization.

Although the absolute emission reductions observed for a single vehicle may appear modest (approximately 6%), it is important to emphasize that these results refer to an individual BEV. When the analysis is extended to a large fleet of EVs, as mentioned in Section 3.4, the cumulative impact of environmentally driven charging optimization becomes substantial, preventing a potential increase of about 7% in the total passenger transport sector. From this perspective, the proposed $V1G_{CO2}$ strategy represents a scalable and easily implementable approach that complements existing grid-oriented smart charging paradigms, thereby contributing to the decarbonization of the transportation sector.

It should be noted, however, that this study assumes that the additional electrical load associated with charging a single BEV does not significantly affect the national electricity production mix. Building on the obtained outcomes, even in the worst-case scenario (February 6th), the energy required for charging is approximately 20 kWh. This amount is negligible when compared to the typical scale of power system operation and is unlikely to influence generation dispatch decisions or activate additional generation capacity. Therefore, the use of hourly average grid emission factors is considered appropriate at the individual vehicle level. This assumption may no longer hold in the case of large-scale EV adoption, where coordinated charging could influence generation dispatch and require the activation of flexible power plants. In this context, the optimization process should be extended to account for the marginal electricity generation mix and the corresponding marginal CO_2 emissions factor, as discussed in Section 2.3. It is also important to note that the charging window considered in this work predominantly falls during nighttime hours, when the electricity system typically operates with lower demand and flexible resources are available to modulate their output, except for the early evening period around 8:00 PM, which coincides with the upward ramp of the system load. As a result, even in the case of a large-scale deployment of EVs, additional charging demand would not necessarily imply the commissioning of new generation units, but could instead be accommodated through adjustments in the operation of existing flexible assets, such as pumped-storage hydroelectricity, leading to a reduction in the CO_2 emission factor.

Finally, it should be noted that the proposed $V1G_{CO2}$ strategy is general and transferable across different national electricity systems, although the achievable emission reduction potential depends on the temporal variability of the local generation mix.

ACKNOWLEDGMENT(S)

This work was supported by the European Union – Next Generation EU, Mission 4, Component 2, Investment Line 1.3: 'Research Program of the Extended Partnership – Network 4 Energy Sustainable Transition (NEST)', Italian Ministry of University and Research (MUR), Identification Code: PE00000021 – Spoke 7 'Smart Sector Integration', CUP: E63C22002160007.

NOMENCLATURE

Symbols

E	electrical energy required for BEV charging	[kWh]
Q	energy stored in the battery	[kWh]
sched	daily charging schedule	[kWh]
T	temperature	[°C]

Greek letters

α	CO_2 emission factor of the power grid	[gCO_2/kWh]

Subscripts and superscripts

CO_2	Carbon dioxide emissions
d	Day index
in	Initial
Max	Nominal capacity
P	Rated charging power
r	Travelled distance
Residual	Residual energy
TE_F	Thermoelectric power plants fuelled by fossil fuels
TE_F +B	Thermoelectric power plants fuelled by fossil fuels and biofuels
TE_F +RES	Thermoelectric power plants, including fossil-based and renewable electricity generation

Abbreviations

BESS	Battery Energy Storage System
BEV	Battery Electric Vehicle
ENTSO-E	European Network of Transmission System Operators for Electricity
EU	European Union
EV	Electric Vehicle
FCEV	Fuel Cell Electric Vehicle
HEV	Full Hybrid Electric Vehicle
GME	Italian electricity market operator (Gestore Mercati Energetici)
ICEV	Internal Combustion Engine Vehicle
ISPRA	Istituto Superiore per la Protezione e la Ricerca Ambientale
MHEV	Mild Hybrid Electric Vehicle
PHEV	Plug-in Hybrid Electric Vehicle
PUN	Italian National Single Electricity Price (Prezzo Unico Nazionale)
RES	Renewable Energy Source
SOC	State Of Charge
TSO	Transmission System Operator
TTW	Tank-to-Wheel
V1G	Unidirectional Vehicle-to-Grid
$V1G_{CO2}$	Environmentally driven smart charging strategy

V2G Bidirectional Vehicle-to-Grid
WLTP Worldwide Harmonised Light-Duty Vehicles Test Procedure
WTT Well-to-Tank
WTW Well-to-Wheel

REFERENCES

1. The European Green Deal - European Commission., https://commission.europa.eu/strategy-and-policy/priorities-2019-2024/european-green-deal_en, [Accessed: 04-Dec-2025].
2. Transport - Energy System – IEA, https://www.iea.org/energy-system/transport, [Accessed: 04-Dec-2025].
3. CO_2 emissions from cars: facts and figures (infographics) | Topics | European Parliament., https://www.europarl.europa.eu/topics/en/article/20190313STO31218/co2-emissions-from-cars-facts-and-figures-infographics, [Accessed: 04-Dec-2025].
4. Greenhouse gas emissions from transport in Europe | Indicators | European Environment Agency (EEA)., https://www.eea.europa.eu/en/analysis/indicators/greenhouse-gas-emissions-from-transport [Accessed: 04-Dec-2025].
5. Alternative fuels for sustainable mobility in Europe - Mobility and Transport., https://transport.ec.europa.eu/transport-themes/clean-transport/alternative-fuels-sustainable-mobility-europe_en, [Accessed: 04-Dec-2025].
6. Directive - 2014/94 - EN - EUR-Lex., https://eur-lex.europa.eu/eli/dir/2014/94/oj/eng, [Accessed: 04-Dec-2025].
7. Regulation - 2019/631 - EN - EUR-Lex., https://eur-lex.europa.eu/eli/reg/2019/631/oj/eng, [Accessed: 04-Dec-2025].
8. Italy, Germany join carmakers in call to rethink internal combustion engine ban | Euronews, https://www.euronews.com/my-europe/2024/09/25/italy-germany-join-carmakers-in-call-to-rethink-internal-combustion-engine-ban, [Accessed: 04-Dec-2025].
9. M. M. Rahman, Y. Zhou, J. Rogers, V. Chen, M. Sattler, and K. Hyun, A comparative assessment of CO_2 emission between gasoline, electric, and hybrid vehicles: A Well-To-Wheel perspective using agent-based modeling, *J. Clean. Prod.*, vol. 321, pp 128931, 2021, https://doi.org/10.1016/J.JCLEPRO.2021.128931.
10. P. Bastida-Molina, E. Hurtado-Pérez, E. Peñalvo-López, and M. Cristina Moros-Gómez, Assessing transport emissions reduction while increasing electric vehicles and renewable generation levels, *Transp. Res. D Transp. Environ.*, vol. 88, pp 102560, 2020, https://doi.org/10.1016/J.TRD.2020.102560.
11. R. Kataoka, K. Ogimoto, Y. Iwafune, and T. Nishi, Does BEV always help to reduce CO_2 emission? impact of charging strategy, *Transp. Res. D Transp. Environ.*, vol. 129, pp 104124, 2024, https://doi.org/10.1016/J.TRD.2024.104124.
12. B. Xu, A. Sharif, M. Shahbaz, and K. Dong, Have electric vehicles effectively addressed CO_2 emissions? Analysis of eight leading countries using quantile-on-quantile regression approach, *Sustain. Prod. Consum.*, vol. 27, pp 1205–1214, 2021, https://doi.org/10.1016/J.SPC.2021.03.002.
13. E. Marrasso, C. Martone, G. Pallotta, I. Perugini, C. Roselli, and M. Sasso, Environmental Impact of Charging Private Battery Electric Vehicles Starting from Real Carbon Dioxide Emissions Factors for Electricity Production in Italy, *Conference Proceedings - 2025 IEEE International Conference on Environment and Electrical Engineering and 2025 IEEE Industrial and Commercial Power Systems Europe, EEEIC / I and CPS Europe 2025*, 2025, https://doi.org/10.1109/EEEIC/ICPSEurope64998.2025.11169245.

14. D. Mehlig, H. ApSimon, and I. Staffell, Emissions from charging electric vehicles in the UK, *Transp. Res. D Transp. Environ.*, vol. 110, pp 103430, 2022, https://doi.org/10.1016/J.TRD.2022.103430.
15. F. Ceglia, E. Marrasso, C. Roselli, and M. Sasso, Time-evolution and forecasting of environmental and energy performance of electricity production system at national and at bidding zone level, *Energy Convers. Manag.*, vol. 265, pp 115772, 2022, https://doi.org/10.1016/j.enconman.2022.115772.
16. M. Noussan, L. Laveneziana, M. Prussi, and D. Chiaramonti, Well-to-wheel greenhouse gas emissions comparison of electricity and biomethane urban buses, *Energy Conversion and Management: X*, vol. 28, pp 101232, 2025, https://doi.org/10.1016/J.ECMX.2025.101232.
17. P. Jochem, S. Babrowski, and W. Fichtner, Assessing CO_2 emissions of electric vehicles in Germany in 2030, *Transp. Res. Part A Policy Pract.*, vol. 78, pp 68–83, 2015, https://doi.org/10.1016/J.TRA.2015.05.007.
18. Ricerca Sistema Energetico (RSE), Impatto delle infrastrutture di ricarica sulla rete elettrica di distribuzione (in Italian, Impact of Charging Infrastructure on the Electric Distribution Network), 2022, https://www.arera.it/fileadmin/allegati/docs/22/449-22alla.pdf, [Accessed: 04-Dec-2025].
19. E. Marrasso, C. Roselli, and M. Sasso, Electric efficiency indicators and carbon dioxide emission factors for power generation by fossil and renewable energy sources on hourly basis, *Energy Convers. Manag.*, vol. 196, pp 1369–1384, 2019, https://doi.org/10.1016/j.enconman.2019.06.079.
20. Z. Zhang, H. Su, W. Yao, F. Wang, S. Hu, and S. Jin, Uncovering the CO_2 emissions of vehicles: A well-to-wheel approach, *Fundamental Research*, vol. 4, no. 5, pp 1025–1035, 2024, https://doi.org/10.1016/J.FMRE.2023.06.009.
21. C. Villante, S. Dell'Aversano, and S. Ranieri, Vehicle Electrification, in *Transition to Sustainable Energy Technologies*, CRC Press, 2025, pp 331–335.
22. N. C. Parker, M. Kuby, J. Liu, and E. B. Stechel, Extreme heat effects on electric vehicle energy consumption and driving range, *Appl. Energy*, vol. 380, pp 125051, 2025, https://doi.org/10.1016/J.APENERGY.2024.125051.
23. J. Bi, Y. Wang, Q. Sai, and C. Ding, Estimating remaining driving range of battery electric vehicles based on real-world data: A case study of Beijing, China, *Energy*, vol. 169, pp 833–843, 2019, https://doi.org/10.1016/J.ENERGY.2018.12.061.
24. B. De Filpo, CONTRIBUTO POTENZIALE DELLA RICARICA BIDIREZIONALE DEI VEICOLI ELETTRICI ALL'EFFICIENZA E ALLA DECARBONIZZAZIONE DEL SISTEMA ELETTRICO ITALIANO (in Italian, Potential Contribution of Bidirectional Electric Vehicle Charging to the Efficiency and Decarbonization of the Italian Power System), 2024, https://www.arera.it/fileadmin/allegati/docs/24/417-2024-I-eel.pdf, [Accessed: 13-Dec-2025).
25. DACIA, SPRING : simulatore autonomia - Dacia. (in Italian, SPRING: Driving Range Simulation Tool – Dacia), https://www.dacia.it/gamma-ibrida-ed-elettrica/spring-city-car/simulatore-tempo-ricarica.html#autonomy, [Accessed: 13-Dec-2025].
26. PVGIS tools - The Joint Research Centre: EU Science Hub., https://joint-research-centre.ec.europa.eu/photovoltaic-geographical-information-system-pvgis/pvgis-tools_en, [Accessed: 15-Dec-2025].
27. UNRAE, L'automobile: italiani a confronto, (in Italian, The Automobile: Italians in Comparison), 2022, https://unrae.it/files/Studio%20UNRAE%20L_automobile%20Italiani%20a%20confronto_6336ab4170253.pdf?utm, [Accessed Apr. 29, 2025].

28. Migliori Wallbox di ricarica domestica. (in Italian, Best Home Charging Wallboxes), https://senec.com/it/le-migliori-wallbox-la-ricarica-domestica-guida-completa-alla-scelta, [Accessed: 15-Dec-2025].
29. Installazione wallbox domestica per ricaricare la tua auto elettrica | VIVI energia. (in Italian, Home Wallbox Installation for Charging Your Electric Vehicle | VIVI energia), https://www.vivienergia.it/efficienza/wallboxcasa, [Accessed: 15-Dec-2025].
30. Richiedi subito il modello di wallbox che preferisci. (in Italian, Request the Wallbox Model You Prefer Now), https://forms.zohopublic.eu/octoenergyitaly1/form/Richiedisubitoilmodellodiwallboxchepreferisci/formperma/0LPFaawRirLCig1I25448cJFPvlKJlchOZlsNTB_wug?utm_source=sito&utm_medium=bottone&utm_medium=bottone&utm_campaign=FastSales_WB&utm_campaign=tecnologie_p, [Accessed: 15-Dec-2025].
31. WallBox Domestiche per ricaricare l'auto a casa tua | Eni Plenitude. (in Italian, Home Wallboxes for Charging Your Car at Home | Eni Plenitude), https://eniplenitude.com/mobilita-elettrica/stazione-ricarica-wallbox-residenziale, [Accessed: 15-Dec-2025].
32. Wallbox e stazioni di ricarica auto elettrica per condominio. (in Italian, Wallboxes and Electric Vehicle Charging Stations for Apartment Buildings), https://www.eon-energia.com/e-mobility/eon-drivesmart-condominio.html, [Accessed: 15-Dec-2025].
33. Colonnina di ricarica auto Wallbox ABB 7.4 kW | IrenLuceGas. (in Italian, ABB 7.4 kW Wallbox Electric Vehicle Charging Station | IrenLuceGas), https://www.irenlucegas.it/p/wallbox-abb-ac-7-4-kw-000000000001076233.html, [Accessed: 15-Dec-2025].
34. Waybox: stazione di ricarica domestica | Enel Energia. (in Italian, Waybox: home charging station), https://www.enel.it/it-it/mobilita-elettrica/waybox, [Accessed: 15-Dec-2025].
35. Unione Nazionale Rappresentanti Autoveicoli Esteri, L'AUTO 2024, Jun. 2025,. [Online]. Available: www.unrae.it, [Accessed: 17-Dec-2025]
36. DACIA, City car Spring elettrica 4 posti - Dacia. (in Italian, Dacia Spring 4-seater electric city car), https://www.dacia.it/gamma-ibrida-ed-elettrica/spring-city-car.html, [Accessed: 17-Dec-2025].
37. DACIA, Scheda tecnica DACIA Spring - Dacia media website Italia. (in Italian, DACIA Spring technical specifications - Dacia media website), https://media.dacia.it/scheda-tecnica-dacia-spring/, [Accessed: 17-Dec-2025].
38. AUTOMOTO.IT, Dacia Spring Comfort Plus Electric 45: prezzo e scheda tecnica - Automoto.it. (in Italian, Dacia Spring Comfort Plus Electric 45: Price and Technical Specifications – Automoto.it), https://www.automoto.it/catalogo/dacia/spring/comfort-plus-electric-45/158491#google_vignette, [Accessed: 17-Dec-2025).
39. WLTP Combined Cycle Time - What is it | Electric Mobility | V2C., https://v2charge.com/wltp-combined-cycle/, [Accessed: 18-Dec-2025].
40. O. Izquierdo-Monge, A. Z. V. Bonilla, M. Lafuente-Cacho, P. Peña-Carro, and Á. Hernández-Jiménez, Performance and energy consumption of electric vehicles used in microgrid management: Analysis of the real impact of ambient temperature, *J. Power Sources*, vol. 635, pp 236511, 2025, https://doi.org/10.1016/J.JPOWSOUR.2025.236511.
41. A. Braun and W. Rid, Energy consumption of an electric and an internal combustion passenger car. A comparative case study from real world data on the Erfurt circuit in Germany, *Transportation Research Procedia*, vol. 27, pp 468–475, 2017, https://doi.org/10.1016/J.TRPRO.2017.12.044.
42. Best EV for Winter & Cold Weather Range » 30,000 Car Study., https://www.recurrentauto.com/research/winter-ev-range-loss, [Accessed: 19-Dec-2025].

43. T. Yuksel, M. A. M. Tamayao, C. Hendrickson, I. M. L. Azevedo, and J. J. Michalek, Effect of regional grid mix, driving patterns and climate on the comparative carbon footprint of gasoline and plug-in electric vehicles in the United States, *Environmental Research Letters*, vol. 11, no. 4, pp 044007, 2016, https://doi.org/10.1088/1748-9326/11/4/044007.
44. TERNA, Dati statistici sull'energia elettrica in Italia - 2023 (in Italian, Statistical Data on Electricity in Italy – 2023), https://download.terna.it/terna/ANNUARIO%20STATISTICO%202023_8dd1f6457916183.pd, [Accessed: 21-Dec-2025].
45. ENTSOE, Transparency Platform., https://transparency.entsoe.eu/, [Accessed: 22-Dec-2025].
46. ISPRA, Fattori-di-emissione-produzione-consumo-energia-elettrica – EMISSIONI, (in Italian, Factors-emissions-production-consumption-electricity – EMISSIONS), 2024, https://emissioni.sina.isprambiente.it/fattori-di-emissione-produzione-consumo-energia-elettrica/, [Accessed: 22-Dec-2025].
47. A. D. Hawkes, Estimating marginal CO_2 emissions rates for national electricity systems, *Energy Policy*, vol. 38, no. 10, pp 5977–5987, Oct. 2010, https://doi.org/10.1016/J.ENPOL.2010.05.053.
48. GME, Historical Data. https://www.mercatoelettrico.org/en-us/Home/Results/Electricity/MGP/StatisticalData/HistoricalData, [Accessed: 23, 2026].
49. What is an EV battery state of charge (SOC)? - EV Engineering & Infrastructure. https://www.evengineeringonline.com/what-is-an-ev-battery-state-of-charge-soc/, [Accessed: 24-Dec-2025].
50. M. K. Tran *et al.*, A comprehensive equivalent circuit model for lithium-ion batteries, incorporating the effects of state of health, state of charge, and temperature on model parameters, *J. Energy Storage*, vol. 43, 2021, https://doi.org/10.1016/j.est.2021.103252.
51. J. Leijon, Charging strategies and battery ageing for electric vehicles: A review, *Energy Strategy Reviews*, vol. 57, no. 2, pp 101641, 2025, https://doi.org/10.1016/j.esr.2025.101641.
52. X. Zeng *et al.*, Comparative evaluation of battery charging strategies: Thermal behavior and charging performance, *Int. J. Heat Mass Transf.*, vol. 256, pp 127947, 2026, https://doi.org/10.1016/J.IJHEATMASSTRANSFER.2025.127947.

Paper submitted: 30.12.2025
Paper revised: 11.02.2026
Paper accepted: 18.02.2026